One-Pot Fabrication of K-Doped g-C_3N_4/SiO_2Composite with Enhanced Photocatalytic Activity for Degradation of Tetracycline

Min-keng He, Jin Zhang, Fang-yan Chen*, Ke-keShu, Yu-bin Tang**
[1]*School of Environmental and Chemical Engineering, Jiangsu University of Science and Technology, Zhenjiang, 212003, P .R. China.*
chenfangyan@just.edu.cn*; ybbill@163.com**

(Received on 10th May 2020, accepted in revised form 26th November 2020)

Summary: K-doped g-C_3N_4/SiO_2composite (SiO_2/K-CN) was synthesized by a facile thermal polymerization with potassium chloride, melamine and nano-silica as raw materials. The as-prepared SiO_2/K-CN was characterized by various measures. The photocatalytic activity of SiO_2/K-CN was tested via the photocatalytic degradation of tetracycline under visible-light irradiation. The results showed that the specific surface area of SiO_2/K-CN catalyst was 28.16m^2/g, which is larger than that of pristine K-doped g-C_3N_4. Both K-doping and silica-combination can reduce the recombination rate of photo-generated electrons-holes pairs and broaden the region of visible light-harvesting. Compared with the pristine K-doped g-C_3N_4 and composite SiO_2/g-C_3N_4, SiO_2/K-CN exhibits distinctly higher photocatalytic activity for degradation of tetracycline. The enhanced photocatalytic performance of SiO_2/K-CN is attributed to the increased specific surface area and the synergistic effect of K-doping and silica-combination in both accelerating separation of charged carries and improving visible light-absorption. During photocatalytic degradation of tetracycline, superoxide radicals play the most important role, followed by holes.SiO_2/K-CN complex has excellent stability and shows promising application in photocatalytic degradation of organic contaminants in water.

Keywords：Graphitic carbon nitride, K-doping, Silica, Composite, Photocatalyst, Tetracycline.

Introduction

Photocatalytic degradation of organic pollutants in water is one of the important research hot spots in field of water treatment owing to its advantages of low energy consumption, low cost, no secondary pollution and soon. In the past decades, various kinds of semiconductors, especially the semiconductors with response to visible-light have been investigated as photocatalysts for degradation of organic pollutants[1-7].Of all the photocatalysts, polymer semiconductor graphitic carbon nitride (g-C_3N_4) has attracted lots of attention in water splitting, degradation of organic contaminant and reduction of carbon dioxide due to absorption of visible-light, highly chemical stability and the distinct redox capability of the photo-produced holes and electrons[8-11].However, Graphitic carbon nitride generally shows some shortcomings, such as limited absorption region to visible-light, low specific surface area and high recombination rate of photo-generated carries[12-14].Thus, various kinds of modification strategy, including element doping, morphology control and combining with other materials to construct composite catalysts have been explored to overcome above-mentioned drawbacks and resultantly optimize the photocatalytic ability of g-C_3N_4[15-17].Element doping has been proven to be an effective modification method. Usually, incorporation of the non-metal elements such as I, N, S, O, F, C, B and P into framework of g-C_3N_4 have been demonstrated to regulate energy band structure and extend absorption region of visible-light, resulting in higher photocatalytic activity [18-23]. The metals have been doped into g-$C_3N_4$to accelerating the migration and separation of photo-induced charges for improving photocatalytic performance [24, 25]. Especially, K has been considered as desired dopant into the structure of g-C_3N_4 [26, 27].For instance, Xiong *et al* have confirmed that K-doped g-C_3N_4 exhibits remarkably enhanced photocatalytic activity for NO removal, which was far superior to Na-doped g-C_3N_4 [28].Composite structure could improve photocatalytic activity via adjusting bands gap and inhibiting recombination of photo-induced charges. Generally, some metallic oxide semiconductors, such as TiO_2, ZnO and Fe_2O_3 have been employed to combine with g-C_3N_4 as to improving the photocatalytic activity [29-32]. Moreover, silica, as an insulator, has also been used to combine with g-C_3N_4 for enhancing photocatalytic performance because the coexistence of silica not only promote separation of

*To whom all correspondence should be addressed.

photo-induced electron-hole pairs but also bring about increase in specific surface area of C_3N_4[33-35].

Given that both element-doping and composite construct are all effective strategies for improving the photocatalytic performance of g-C_3N_4. It can be inferred that coupling element-doping and composite construct would further enhance the photocatalytic activity of g-C_3N_4. Herein, we report a g-C_3N_4 based composite with simultaneous K-doping and combining with SiO_2. The photocatalytic performance of K-doped g-C_3N_4/$SiO_2$was evaluated for degradation of tetracycline. And the synergistic effect of K-doping and combining with silica on the photocatalytic activity of g-C_3N_4 was explored.

Experimental

Chemicals

Melamine, potassium chloride, tetracycline hydrochloride, L(+) ascorbic acid, isopropanol, potassium iodide were analytical grade, obtained from SinopharmGroup Chemical Reagent Co., Ltd.Nano-silica was in diameter of 15 nm and purchased from Shanghai Aladdin Biochemical Technology Co., Ltd.

Preparation of K-doped g-C_3N_4/SiO_2(SiO_2/K-CN)

The mixture of potassium chloride and melamine in the mass ratio of 1:20 and a given amount of nano-silica (the mass ratio of the mixture of potassium chloride and melamine to nano-silica is 8, 10 and12) were mixed in a crucible and dried at 60 ℃. The crucible was put into a muffle furnace, heated to 520 °C at a heating rate of 15 °C/min, held for 4 h. Then the product was cooled naturally to room temperature and ground to obtain composite K-doped g-C_3N_4/SiO_2, labeled as X-SiO_2/K-CN (X represents the mass ratio of the mixture of potassium chloride and melamine to nano-silica, X=8, 10, 12).

Preparation of K-doped g-C_3N_4(K-CN)

A mixture of potassium chloride and melamine inthe mass ratio of 1:20 was dried in at 60°C.Then the mixed solid was placed into a muffle furnace, heated to 520 ℃ at a heating rate of 15 °C / min, held for 4 h. The product was cooled naturally to room temperature and ground to obtain doped g-C_3N_4, labeled as K-CN.

Preparation of g-C_3N_4/SiO_2 (SiO_2/CN)

Nano-silica and melamine were mixed at the mass ratio of 1:10 in a crucible and dried at 60°C. Then, mixed solids were placed into a muffle furnace, heated to 520 °C at a heating rate of 15 °C / min, held for 4 h. The product was cooled naturally to room temperature and ground. Thecomposite g-C_3N_4 /SiO_2 sample is obtained and marked as SiO_2/CN.

Characterization of catalyst

The crystal phase of the samples was analyzed by XRD patterns obtained on D8 advantage X-ray diffractometer (Bruker, Germany) with Cu-Ka radiation source (λ=1.5406 Å) at 40Kv, 40mA The morphology of the samples was characterized by S-4800 field emission scanning electron microscope(Hitachi, Japan) at operating voltage of 15kV. The Fourier transformed infrared (FT-IR) spectrum of as-prepared catalysts was recorded on a NEXUS670 Fourier transform infrared spectrometer (Nicolet, US) at air atmosphere and scanning range of 350-4000cm^{-1}.The elemental composition and chemical state of the obtained products were measured by ESCALAB250i X-ray photoelectron spectroscopy (XPS) (Thermo Fisher Scientific Inc., UAS). The specific surface area, pore size and pore volume of the samples were determined by N_2adsorption-desorption isothermobtained on anAutosorb-1-c sorption analyzer (Quantachrome, USA).UV-vis diffuse reflectance spectra were collected on a UV-2550 UV-vis spectrophotometer (Shimadzu, Japan) with $BaSO_4$ as reflectance standard. The photoluminescence spectra of the catalysts were observed on a Fluorescence spectrometer (Hitachi, Japan)at the excitation wavelength of 385 nm.The transient photocurrent response was carried out on the CHI660D electrochemical workstation(Chenhua Instrument, China)with Na_2SO_4 solution of 0.2mol/L as electrolyte, 300W arc beam(λ>420nm)as light source.

Photocatalytic degradation

Tetracyclinewas chosen as model pollutant to evaluate the photocatalytic activity of the as-prepared catalysts.50mg photocatalysts were dispersed in aqueous solution of the tetracycline hydrochloride (100mL, 10mg/L) and stirred in darkness for 60min to achieve adsorption-desorption equilibrium. Then the suspension was exposed to a 300W xenon lamp with a 420 nm cut-off filter. At a given intervals, 4.5 mLof solution was sampled and centrifuged to separate the photocatalysts. The concentration of tetracycline in supernatant was determined according to the

absorbance at wavelength of 357nm.

Results and discussion

XRD spectra

The XRD spectra of K-CN, X-SiO_2/K-CN (X=8, 10, 12) and SiO_2/CN are given in Fig. 1.As shown in Fig.1, the diffraction peaks at 12.8°and 27.4°are the characteristic peaks of (100) and (002) crystal plane of the g-C_3N_4, belonging to the repeating of in-plane N-bridged tri-s-triazine units and the interlayer stacking of conjugatedgraphite-like segments, respectively[36,37].The five samples all show similar diffraction peaks at 12.8°and 27.4°, indicating that both K-doping and combining with SiO_2 does not change the crystalline phase of g-C_3N_4.

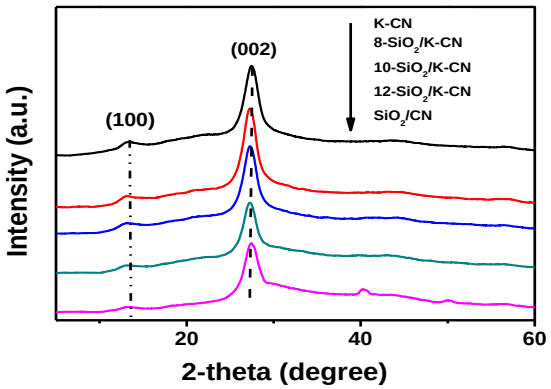

Fig. 1: XRD patterns of K-CN, SiO_2/CN and X-SiO_2/K-CN (X=8, 10, 12).

FT-IR spectra

Fig. 2 is the infrared spectra of the as-prepared photocatalysts. As given in Fig. 2, K-CN, SiO_2/CN and 10-SiO_2/K-CN all exhibit the characteristic peaks of g-C_3N_4 at 794cm^{-1}, 1414cm^{-1}, 1562cm^{-1}, 1247cm^{-1}, 1331cm^{-1} and 3000-3500cm^{-1}. Among these typical peaks, the sharp peak at 794$cm^{-1}$is attributed to out-of-plane bending vibration of triazinering of g-C_3N_4. The adsorption band at 1247cm^{-1} and 1331$cm^{-1}$are assigned to the stretching vibration of C-N group, and the peak located at 1414cm^{-1} and 1562$cm^{-1}$is due to the stretching vibration of C=N[38]. The broad band at 3000-3300 cm^{-1} perhaps belongs to the terminal N-H stretching vibration of g-C_3N_4. The absorption peak at 467.4cm^{-1}found in the infrared spectra of 10-SiO_2/K-CN and SiO_2/CNis assigned to the bending vibration of O-Si-O, which proves the existence of SiO_2 in 10-SiO_2/K-CN and SiO_2/CN. Additionally, a new absorption peak at 2160$cm^{-1}$is observed in the infrared spectra of 10-SiO_2/K-CN and K-CN, which corresponds to the stretching vibration of N-K bond[39], indicating K element is successfully inserted into the skeleton of g-C_3N_4.

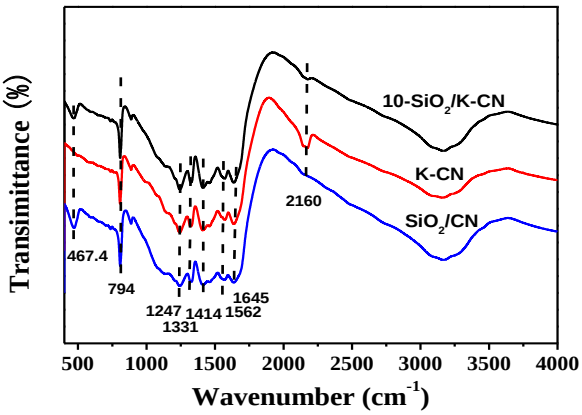

Fig. 2: FT-IR spectra of K-CN, SiO_2/CN and X-SiO_2/K-CN(X=8, 10, 12),

X-photoelectron spectroscopy (XPS)

Fig. 3 shows the XPS spectrum of 10-SiO_2/CN. As can be seen from Fig. 3, O1s, C 1s, N 1s and Si 2P are observed in the survey spectrum (Fig. 3(a)), suggesting that sample 10-SiO_2/K-CN contains O, C, N, Si and K elements. In the high resolution spectrum of C 1s (Fig. 3(b)), C1s spectrum can be deconvoluted into two peaks at 288.17eV and 284.7eV. Of them, the former corresponds to sp2 hybridized carbon atom from the triazine ring of g-C_3N_4[40], and the latter is perhaps due to surface amorphous carbon or sp2 C-C of the catalyst [28, 41]. In the high resolution spectrum of N 1s (Fig. 5(c)), the binding energy at 398.6eV, 399.5eV and 400.5eV are attributed to C-N=C, tertiary nitrogen N-$(C)_3$ and C-N-H, respectively, while the peaks at 404.4eV is due to positive charge localization or charging effects about the π-excitations in heterocycles[37, 39].Fig. 6(d) shows the high resolution spectrum of K 2p,and the binding energy of 293.04eV and 295.08eV are ascribed toK2p3/2 and K2p1/2 , which is similar to that of K-N in potassium azide (KN_3) [39], confirming successful K-doping into framework of g-C_3N_4 and the formation of N-K bond. In Fig.6(e), the high resolution spectrum of O1s at 533.2eVcorresponds to element oxygen from nano-SiO_2.In Fig. 5(f), the peak at the binding energy of 104.06eV is indexed to Si^{4+} from the nano-silica[35].

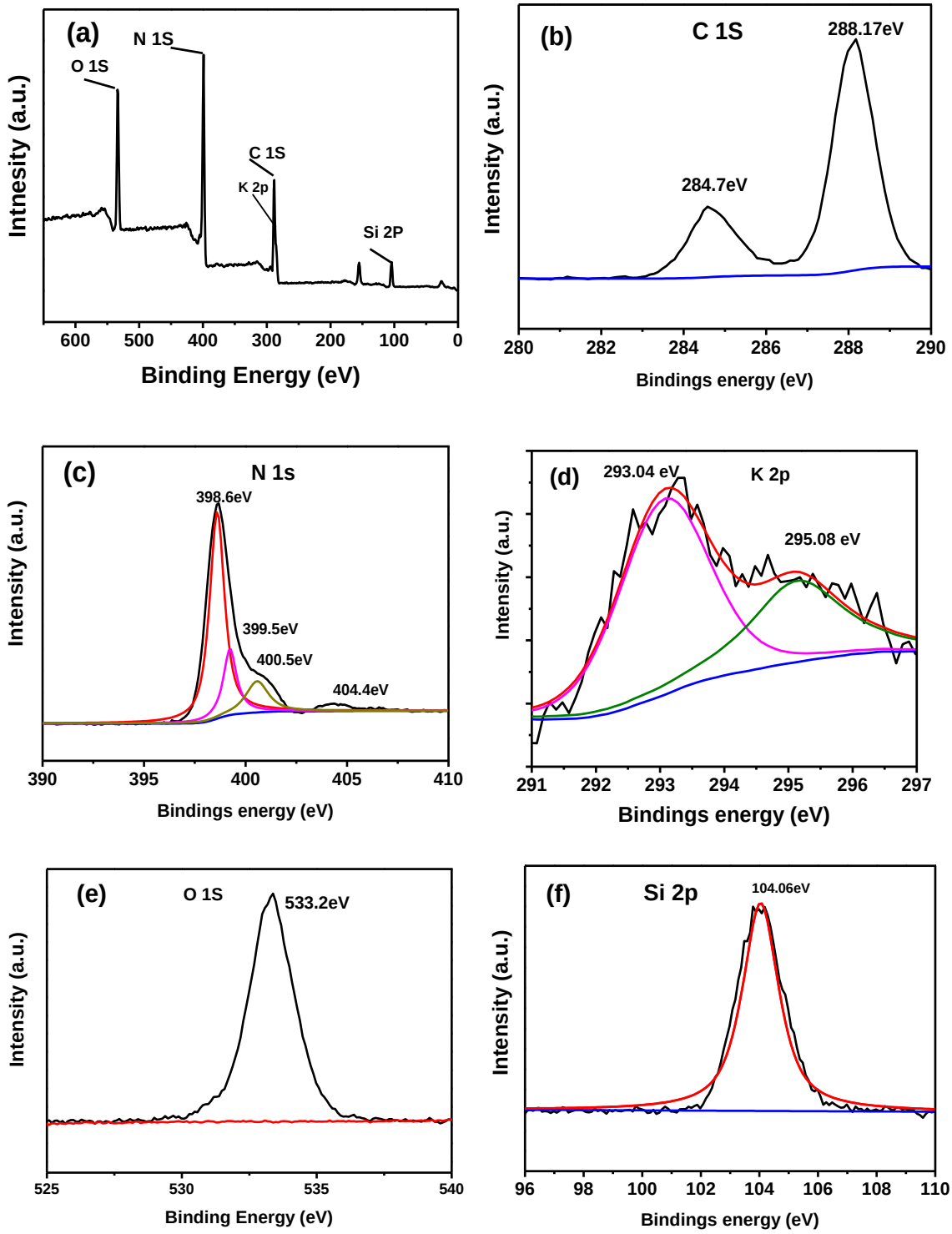

Fig. 3: XPS spectra of 10-SiO_2/K-CN.

SEM

Fig. 4 indicates the SEM images of 10-SiO_2/K-CN and K-CN. As shown in Fig. 4, both K-CN and 10-SiO2/K-CN are all blocky. However, 10- SiO_2/K-CN appears more rough and loose surface than the separate K-doped g-C_3N_4, which will be further confirmed by the specific area shown in table 1.

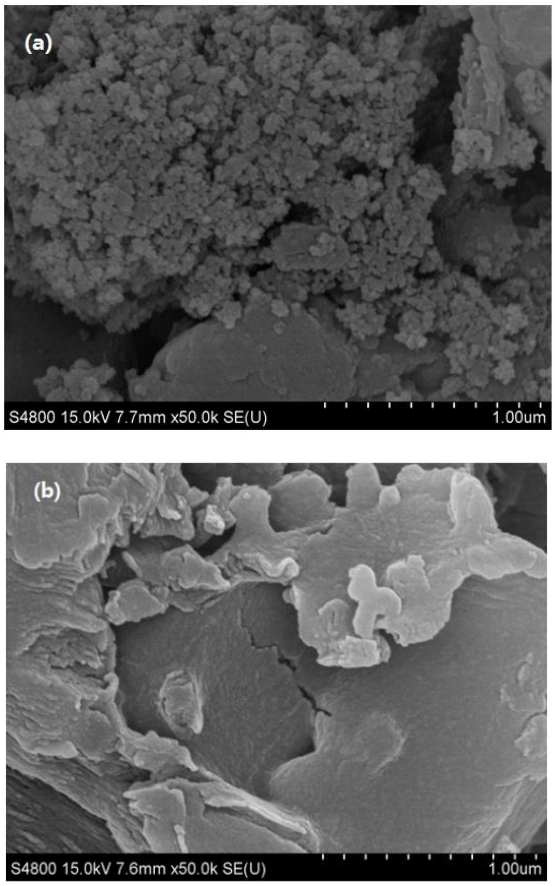

Fig. 4: SEM of K-CN (a) and 10-SiO_2/K-CN (b).

Table-1: Specific surface area and pore volume of the catalysts.

Samples	Specific surfaceArea (cm^2/g)	Pore volume (cm^3/g)
10-SiO_2/K-CN	28.156	0.0950
10-SiO_2/CN	46.389	0.1595
K-CN	11.730	0.0329

N_2 adsorption-desorption

Fig. 5 is the nitrogen adsorption-desorption isotherm and pore size distribution of K-CN and 10-SiO_2/K-CN. On basis of BET adsorption-desorption model, the specific surface area and pore volume of the samples were calculated and listed in Table-1. As shown in Table-1, 10-SiO_2/K-CN exhibits larger porosity and specific surface areas than K-CN. It is suggested that combination of SiO_2 can contribute to improve specific surface of the K-doped g-C_3N_4. Nevertheless, it is noted that the specific surface areas and porosity of 10-SiO_2/K-CN is smaller than SiO_2/CN, suggesting K-doping results in decrease in the specific surface areas of SiO_2/K-CN. It is perhaps because the K-doping enhance interaction and degree of polymerization between carbon nitride sheets and resultantly reduces the specific surface area [39].

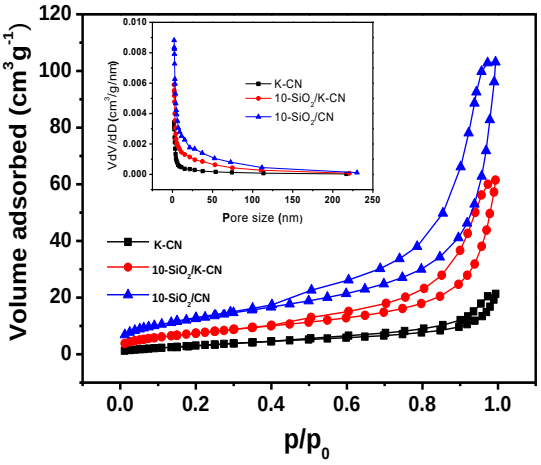

Fig. 5: Nitrogen adsorption-desorption isotherm and pore size distribution.

UV-visible diffuse reflectance spectrum

Fig. 6(a) shows the UV-vis spectra of samples 10-SiO_2/K-CN, K-CN and SiO_2/CN.It can be seen from Fig. 6(a) that compared with K-CN, the visible-adsorption edge of composite 8-SiO_2/K-CN, 10-SiO_2/K-CN and 12-SiO_2/K-CN undergo evident red-shift. Furthermore, the red-shift increases with increased content of SiO_2 in composite SiO_2/K-CN, indicating that the existence of SiO_2 in composite SiO_2/K-CN can result in extensive visible-light adsorption of the composite. Similarly, compared with the composite SiO_2/CN, The UV-Vis spectra of SiO_2/K-CN also show obvious red-shift, suggesting that K-doping can broaden the region of visible light-harvesting and thus enhance the strength of visible-light adsorption of SiO_2/CN. Therefore, it can be concluded that K-doping and SiO_2 recombination

have synergistic effect on enhancing the absorption of visible-light of SiO_2/K-CN.

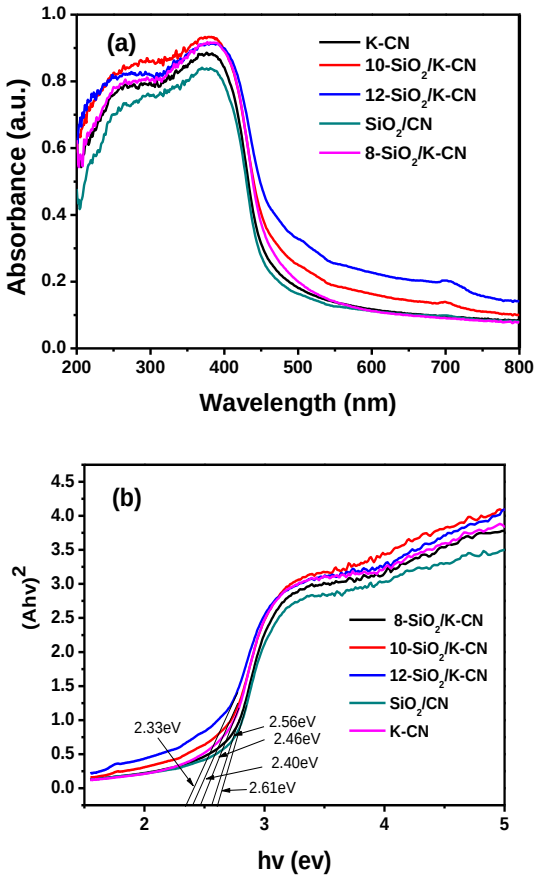

Fig. 6: UV-vis diffuse reflectance spectra (a) and the plots of $(\alpha hv)^{1/2}$versushv(b).

According to Tauc formula $\alpha hv = A(hv-E_g)^{1/2}$, the band gaps of a semiconductor can be estimated by the intercept of the tangents to the plots of $(\alpha hv)^{1/2}$ versus hv,where A, α, hv, E_g are a constant, the absorption coefficient, photo energy and the band gap, respectively[28]. Fig. 6(b) gives the plots of $(\alpha hv)^2$ versus (hv) for the as-synthesized photocatalysts. On the basis of Fig. 6(b), the band gap of K-CN, 8--SiO_2/K-CN, 10-SiO_2/K-CN, 12--SiO_2/K-CN and SiO_2/CN were obtained to be 2.56eV, 2.46eV, 2.40eV, 2.33eV and 2.61eV, respectively. Compared with K-CN, the band gap of SiO_2/K-CN is narrower and decrease with increasing the content of SiO_2 in composite SiO_2/K-CN. It is because nano silica possesses band defects due to its over-small size,which leads to a smaller band gap as it is combined with a semiconductor photocatalyst [42]. Additionally, the composite SiO_2/K-CN with K-doping own less band gap than non-doping composite SiO_2/CN. Comparison of band gap suggested that both K-doping and the SiO_2 combination narrow the band gap of SiO_2/K-CN.

Photoluminescence(PL) spectrum

To explore the recombination probability of photo-generated electron-hole pairs of the as-prepared catalysts, the photoluminescence performance test of K-CN, 10-SiO_2/K-CN and SiO_2/CN were conducted and presented in Fig. 7. As can be seen from Fig. 7, PL intensity of 10-SiO_2/K-CN is weaker than that of both K-CN and SiO_2/CN, indicating that 10-SiO_2/K-CN exhibits lower recombination rate of photo-induced electron-hole pairs, and K-doping and SiO_2 combination show a synergistic effect on inhibiting the recombination of photo-induced charges in SiO_2/K-CN. However, the PL intensity of 10-SiO_2/K-CN is significantly weaker than that of SiO_2/CN but slightly weaker than that of K-CN, suggesting that K-doping produced more marked effect on inhibiting the recombination of photo-generated charges compared with SiO_2 combination.

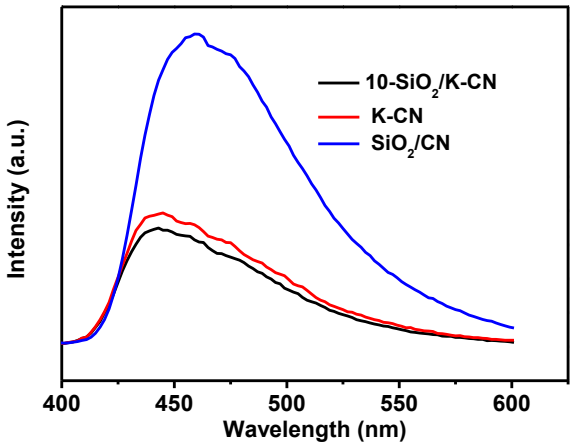

Fig. 7: Photoluminescence spectra of K-CN, 10-SiO_2/K-CN and SiO_2/CN.

Transient photocurrent responses

To further verify the separation and transfer of the photo-produced electron-hole pairs in SiO_2/K-CN, the Transient photocurrent responses under visible-light irradiation was tested and shown in Fig. 8. It is observed form Fig.8 that 10-SiO_2/K-CN

exhibits the highest photocurrent, indicating efficient separation of photo-induced charges in 10-SiO_2/K-CN. This result is in accordance with PL result. Moreover, the fact that the photocurrent of 10- SiO_2/K-CN is greater than that of both K-CN and SiO_2/CN further confirm the synergistic effect of K-doping and silica-combination on expediting the separation and transfer of photo-induced charges in SiO_2/K-CN.Because the new N-K bond formed between K^+ and -NH_2 or -NH group in g-C_3N_4 can link triazine rings together to expand the π-conjugate system of g-C_3N_4 and thus reduce the adjacent layers of energy barrier[39]. As a result, the migration of photo-produced electrons is promoted and then recombination of electrons and holes is inhibited. In addition, Nano-SiO_2 in SiO_2/K-CN own impurity energy level due to the existence of defects [33], which makes the photo-generated electrons transfer from the conduction band of g-C_3N_4 to the impurity energy level of SiO_2 and thus hinder the recombination of photo-generated electrons and holes.

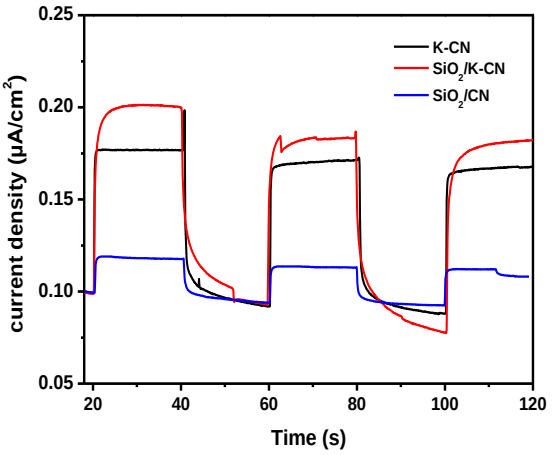

Fig. 8: Transient photocurrent response of K-CN, SiO_2/CN and 10-SiO_2/K-CN under visible-light irradiation.

Photocatalytic performance

The photocatalytic activity of the prepared material was evaluated by photocatalytic degradation of Tetracycline hydrochloride (TC)under visible-light. Fig. 9(a) gives the degradation ratio of TC. As presented in Fig. 9(a), within 120 min, the degradation efficiencies of TC over SiO_2/CN, K-CN, 8-SiO_2/K-CN, 10-SiO_2/K-CN and 12-SiO_2/K-CN are 52.4%, 57.9%, 61.1%, 68.6% and 67.1%, respectively. The visible-light-driven photocatalytic activity of X-SiO_2/K-CN(X=8, 10, 12) is higher than that of K-CN and SiO_2/CN, revealing the synergistic effect of K-doping and silica-combination on improving the activity of SiO_2/K-CN. Of the X-SiO_2/K-CN(X=8, 10, 12), 10-SiO_2/K-CN exhibits the highest activity.

Generally, the photocatalytic degradation of organic pollutants follows apparent first-order kinetics equation: ln (C_t/C_0)=-kt, where, C_t and C_0 are the concentration of RhB at t time and initial time, respectively, k is apparent reaction constant. Fig. 9 (b) gives plots of ln (C_t/C_0) vs. t of the obtained photocatalysts. The values of k are obtained from the gradient of curve in Fig. 9(b) and listed in Table-2. As can be seen from Table-2 that x-SiO_2/K-CN (X=8, 10, 12) exhibits significant higher rate constant for degradation of tetracycline than K-CN and SiO_2/CN. Moreover, degradation rate constant of tetracycline over10-SiO_2/K-CN is 1.54 and 1.39 times as high as that over K-CN and SiO_2/CN, respectively. It is further confirmed that nano-silica and the K-doping show synergistic effect in enhancing the photocatalytic activity of X-SiO_2/K-CN for degradation of tetracycline.

Table-2: Kinetic constants and regression coefficients of degradation of tetracycline hydrochloride.

Samples	K(min^{-1})	R^2
SiO_2/CN	0.00603	0.9945
K-CN	0.00663	0.9899
8-SiO_2/K-CN	0.00771	0.9878
10-SiO_2/K-CN	0.00925	0.9163
12-SiO_2/K-CN	0.00866	0.9836

Fig.9(c) shows the degradation of tetracycline as the 10-SiO_2/K-CN was recycled for 4 times. It can be observed from Fig. 9(c) that the photocatalytic degradation efficiency of tetracycline over 10-SiO_2/K-CN decreased a little from 66.1% to 60.6% after 10-SiO_2/K-CN was reused for 4 cycles. It is suggested that 10-SiO_2/K-CN own apparent stability, showing potential practical application.

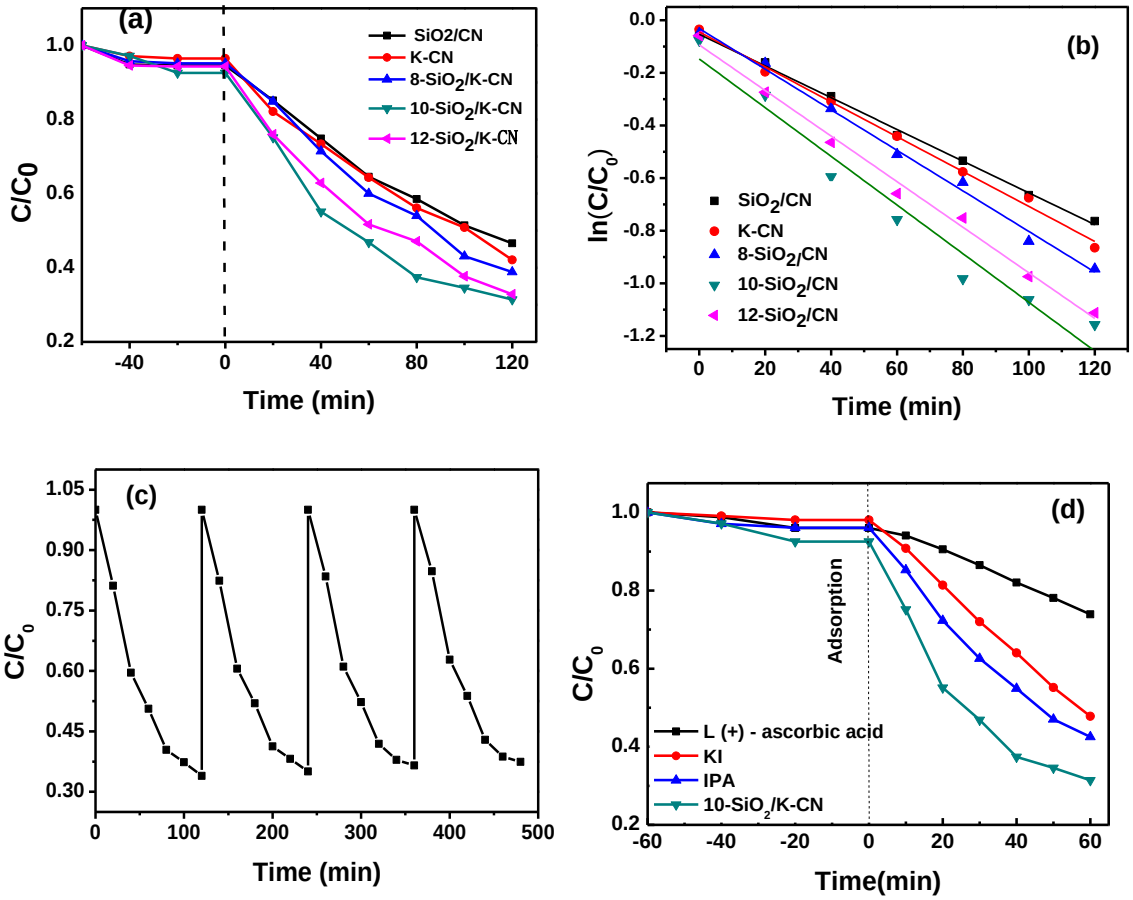

Fig. 9: (a) Photocatalytic degradation of tetracyclineunder visible light, (b)Kinetic curve of degradation of tetracycline, (c) Recycling runs of$X\text{-}SiO_2/CN$ for degradation of tetracycline and (d) photocatalytic activity of $10\text{-}SiO_2/K\text{-}CN$ for degradation in the presence of different radical scavenger

Fig. 9(d) gives the degradation of tetracycline in the presence of L (+)-ascorbic acid, potassium iodide (KI) and isopropanol (IPA) which are used as scavenger for superoxide radicals($\bullet O^{2-}$), holes (h^+) and hydroxyl radicals(•OH), respectively.As shown in Fig. 9(d), the decrease in photocatalytic activity is most significant when L (+)-ascorbic acid was added in tetracycline solution. Addition of KI results in more decreased degradation rates of tetracycline than IPA. It is indicated that superoxide radicals are main active species for degradation of tetracycline, followed by holes, and hydroxyl radicals play a minor role in degradation of tetracycline.

Conclusion

The composite catalyst K-doped $g\text{-}C_3N_4/SiO_2(SiO_2/K\text{-}CN)$ was successfully synthesized by facile thermal polymerization by using nano-silica, melamine and potassium chloride as raw materials. As the mass ratio of potassium chloride to melamine is 1:20 and the mass ratio of the mixture of potassium chloride and melamine to silica is 10:1, the as-prepared composite $10\text{-}SiO_2/K\text{-}CN$ shows the highest photocatalytic activity. The specific surface area of $10\text{-}SiO_2/K\text{-}CN$ is 28.16m^2/g, which is higher than that of K-doped $g\text{-}C_3N_4$(12.58m^2/g) and lower than that of $g\text{-}C_3N_4/SiO_2$ (46.39m^2/g), silica-combination play an important role in increasing the specific surface area of the composite catalyst. Both K-doping and addition of SiO_2 can reduce the recombination rate of photo-generated electrons and holes. Compared with SiO_2/CN and K-CN, $SiO_2/K\text{-}CN$ exhibits enhanced photocatalytic activity for degradation of tetracycline. Within 120 min, 68.6% of tetracycline can be degraded under visible-light irradiation.The superoxide radicals pay

main role in degradation of tetracycline, followed by holes and hydroxyl radicals. The enhanced activity is attributed to the increased specific surface areas and the synergistic effect between K-doping and silica-combination in both promoting the separation of the photo-induced electron-hole pairs and enhancing visible-light absorption. In addition, SiO_2/K-CN shows high stability and reusability, implying potential practical application in decomposition of organic pollutants.

Acknowledgement

This work is supported by Postgraduate Research & Practice Innovation Program of Jiangsu Province, China. (Grant Number: SJKY19_2658).

References

1. F. Y. Chen, Y. M. Liu, X. Zhang, L. N. He and Y. B. Tang, Inorganic-framework Molecularly Imprinted CdS/TiO_2 for Selectively Photocatalytic Degradation of Di (2-ethylhexyl) Phthalate, *J.Chem.Soc.Pak.*, **41,** 308 (2019).
2. M. Wang, J.Ioccozia, L. Sun, C. Lin and Z. Lin, Inorganic-modified Semiconductor TiO_2 Nanotube Arrays for Photocatalysis, *Energ. Environ.Sci.*,**7,** 2182 (2017).
3. W. Y. Jung, K. T. Lim, J. H. Kim, M. S. Lee and S. S. Hong, Synthesis of Pb-substituted $LaCoO_3$ Nanoparticles by Microwave Process and Their Photocatalytic Activity under Visible Light Irradiation. *J. Ind. Eng. Chem.*,**19,** 157 (2013)
4. F. P.Cai, Y. B. Tang, F. Y. Chen, Y. Yan and W. D. Shi, Enhanced Visible-light-driven Photocatalytic Degradation of Tetracycline by Cr^{3+}Doping $SrTiO_3$Cubic Nanoparticles, *RSC Adv.*, **5,**21290(2015).
5. M. Y. Li, Y. B. Tang, W. L. Shi, F. Y. Chen, Y. Shi and H. C.Gu, Design of Visible-light -response Core-shellFe_2O_3/$CuBi_2O_4$Heterojunctions with Enhanced Photocatalytic Activity Towards the Degradation of Tetracycline: Z-scheme Photocatalytic Mechanism Insight, *Inorg. Chem. Front*., **5,** 3148 (2018).
6. J. Xu, B. Y. Luo, W. Gu, Y. P. Jian, F. L. Wu, Y. B. Tang and H. Shen, Fabrication ofIn_2S_3/$NaTaO_3$Composite for Enhancing the Photocatalytic Activity Toward the Degradation of Tetracycline, *New J. Chem.*,**42,**5052(2018).
7. F. Y. Chen, X. Zhang, Y. B. Tang, X. G. Wang and K. K. Shu, Facile and Rapid Synthesis of a Novel Spindle-like Hetero junction $BiVO_4$Showing Enhanced Visible light-driven Photoactivity, *RSC Adv.*, **10,** 5234 (2020).
8. S.Tan, Z.Xing, J.Zhang, Z. Li, X. Wu, J. Cui, J. Kuang, J. Yin and W. Zhou, Meso-g-C_3N_4/g-C_3N_4Nanosheets Laminated Homojunctions as Efficient Visible-light-driven Photocatalysts,*Int. J. Hydrogen Energ.*, **42,** 2596 (2017).
9. H.Ou, W.Zhang, X.Yang, Q. Cheng,G. Liao, H. Xia and D. Wang, One-pot Synthesis of g-C_3N_4-Doped Rich-amine Porous Organic Polymer for ChlorophenolRemoval,*Environ.Sci-Nano*, **5,** 1029 (2017).
10. X.Lu; T. H.Tan,Y. H.Ng andR.Amal, Highly Selective and Stable Reduction of $CO_2$to CO by a Graphitic Carbon Nitride/Carbon Nanotube Composite Electrocatalyst, *Chem.-Eur. J.*,**22,** 11991(2016).
11. J. Jiang, S. Cao, C. Hu, C. Chen,A comparison Study of Alkali Metal-doped g-C_3N_4 for Visible-light Photocatalytic Hydrogen Evolution, *Chinese J. Catal.*,**38,**1981(2017).
12. S. Sun and S. Liang, Recent Advances in Functional Mesoporous Graphitic Carbon Nitride(mpg-C_3N_4) Polymers, *Nanoscale*, **9,** 10544 (2017).
13. K. S. Lakhi, D. H. Park, K. Al-Bahily, W. Cha,B.Viswanathan, J. H.Choy and A. Vinu, Mesoporous Carbon Nitrides: Synthesis, Functionalization and Applications,*Chem. Soc. Rev.*,**46,** 72 (2017).
14. J. Zhang, Y. Chen and X. Wang, Two-dimensional Covalent Carbon Nitride Nanosheets: Synthesis, Functionalization and Applications, *Energ. Environ.Sci.*,**8,** 3092 (2015).
15. S.W. Hu, L.W. Yang, Y. Tian, X.L. Wei, J.W. Ding, J.X. Zhong and P.K. Chu, Simultaneous Nanostructure and Hetero junction Engineering of Graphitic Carbon Nitride via In-situ Ag Doping for Enhanced Photoelectrochemical Activity, *Appl. Catal. B-Environ.*, **163,** 611 (2015).
16. K.C. Christoforidis, T. Montini, E. Bontempi, S. Zafeiratos, J.J. Delgado-Jaen and P. Fornasiero, Synthesis and Photocatalytic Application of Visible-light Active Beta-Fe_2O_3/g-C_3N_4Hybrid Nanocomposites, *Appl. Catal. B-Environ.*, **187,** 171(2016).
17. G. Li, Z. Lian, W. Wang, D. Zhang and H. Li, Nanotube-confinement Induced Size-controllable g-C_3N_4 Quantum Dots Modified Single-crystalline TiO_2Nanotube Arrays for Stable Synergetic Photoelectrocatalysis, *Nano*

Energy,**19,** 446(2016).

18. G.G. Zhang, M.W. Zhang, X.X. Ye, X.Q. Qiu, S. Lin and X.C. Wang, Iodine Modified Carbon Nitride Semiconductors as Visible Light Photocatalysts for Hydrogen Evolution, *Adv. Mater,***26,** 805(2014).
19. Y.J. Zhou, L.X. Zhang, W.M. Huang, Q.L. Kong, X.Q. Fan, M. Wang and J. L. Shi, N-doped Graphitic Carbon-incorporated g-C_3N_4 for Remarkably Enhanced Photocatalytic H_2 Evolution under Visible Light, *Carbon*,**99,** 111 (2016).
20. S.E. Guo, Z.P. Deng, M.X. Li, B.J. Jiang, C.G. Tian, Q.J. Pan and H.G. Fu, Phosphorus-doped Carbon Nitride Tubes with a Layered Micro-nanostructure for Enhanced Visible-light Photocatalytic Hydrogen Evolution, *Angew. Chem.Int.Edit.,***55,** 1830 (2016).
21. Y. Xu and W. D. Zhang, Sulfur/g-C_3N_4 Composites with Enhanced Visible Light Photocatalytic Activity, *Sci. Adv. Mater.* , **6,** 2611 (2014).
22. Z.F. Huang, J.J. Song, L. Pan, Z.M. Wang, X.Q. Zhang, J.J. Zou, W. Mi, X.W. Zhang andL. Wang, Carbon Nitride with Simultaneous Porous Network and O-doping forEfficient Solar-energy-driven Hydrogen Evolution, *Nano Energy*,**12,**646(2015).
23. F. Raziq, Y. Qu, M. Humayun, A. Zada, H.T. Yu and L.Q. Jing, Synthesis of SnO_2/B-PCodoped g-C_3N_4Nanocomposites as Efficient Cocatalyst-free Visible-lightPhotocatalysts for CO_2Conversion and Pollutant Degradation, *Appl. Catal. B:Environ.,***201,**486(2017).
24. K.Li, Z. Huang, X.Zeng, B. Huang, S. Gao and J. Lu, Synergetic Effect of Ti^{3+} and Oxygen Doping on Enhancing Photoelectrochemical and Photocatalytic Properties of TiO_2/g-C_3N_4 Heterojunctions. *Acs Appl. Mater.Inter.,***9,** 11577 (2017).
25. S. Sun, J. Li, J. Cui, X. Gou, Q.Yang,Y. Jiang, S. Liang and Z. Yang, Simultaneously Engineering K-doping and Exfoliation into Graphitic Carbon Nitride (g-C_3N_4) for Enhanced Photocatalytic Hydrogen Production, *Inter. J.Hydrogen Energ.*,**44,** 778 (2019).
26. M. Zhang, X. Bai, D. Liu, J. Wang and Y. Zhu, Enhanced Catalytic Activity of Potassium-doped Graphitic Carbon Nitride Induced by Lower Valence Position. *Appl.Catal.B-Environ.*, **164,** 77(2015).
27. J. Zhao, L. Ma, H. Wang, Y. Zhao, J. Zhang and S. Hu, Novel Band Gap-tunable K-Na Co-doped Graphitic Carbon Nitride Prepared by Molten Salt Method,*Appl. Surf.Sci.,***332,**625 (2015).
28. T. Xiong, W. L. Cen, Y. X. Zhang and F. Dong, Bridging the g-C_3N_4 Interlayers for Enhanced Photocatalysis, *ACS Catal.*, **6,**2462 (2016).
29. J.Shen, Y.Hui, Q.Shen, Y. Feng and Q. Cai. Template-Free Preparation and Properties of Mesoporous g-C_3N_4/TiO_2 Nanocomposite Photocatalyst.*Crystengcomm,***16,** 1868 (2014).
30. W. Yin, S. Bai, Y. J.Zhong andZ. Li, Direct Generation of Fine Bi_2WO_6Nanocrystals on g-C_3N_4Nanosheets for Enhanced Photocatalytic Activity, *Chemnanomat*, **2,** 732 (2016).
31. X.Yuan, Z.Chao, Q.Jing, Q. Tang, Y. Mu and A. K. Du, Facile Synthesis of g-C_3N_4 Nanosheets/ ZnONanocomposites with Enhanced Photocatalytic Activity in Reduction of Aqueous Chromium(VI) under Visible Light,*Nanomaterials*, **6,** 173 (2016).
32. J. Theerthagiri, R. A. Senthil, A. Priyaand M. Jagannathan, Photocatalytic and Photoelectrochemical Studies of Visible-light Active α-Fe_2O_3-g-C_3N_4Nanocomposites.*RSC Adv.*,**4,** 179 (2014).
33. Q. Hao, X. Niu,C.Nie, S. Hao, W. Zou, J. Ge, D. Chen and W. Yao, A Highly Efficient g-C_3N_4/SiO_2Heterojunction: the Role of SiO_2 in the Enhancement of Visible light Photocatalytic Activity, *Phys. Chem. Chem. Phys.*,**18,**31410(2016).
34. B. Lin, C. Xue,X. Yan, G. D. Yang, G. Yang and B. Yang, Facile Fabrication of Novel SiO_2/g-C_3N_4Core-shell NanospherePhotocatalysts with Enhanced Visible Light Activity, *Appl. Surf.Sci.*, **357,**346 (2015).
35. X. Zhang, F. Y. Chen, Y. B. Tang, Y. M. Liu and X. G. Wang, A Rapid Microwave Synthesis of Nanoscale $BiVO_4$/Bi_2O_3@SiO_2 with Large Specific Surface Area and Excellent Visible-light-driven Activity, *Desalin.Water Treat.*,**152,** 99 (2019).
36. J. Lei, C.Ying, L.Wang, Y. Liu and J. Zhang, Highly Condensed g-C_3N_4-modified TiO_2 Catalysts with Enhanced Photodegradation Performance Toward Acid Orange. *J. Mater.Sci.*,**50,** 3467(2015).
37. Y. Tan, Z. Shu, J. Zhou, T. Li, W. Wang and Z. Zhao, One-step Synthesis of Nanostructured g-C_3N_4/TiO_2Composite for Highly Enhanced Visible-light Photocatalytic H_2Evolution. *Appl.Catal.B-Environ.,* **230,** 260(2018).
38. X. Wang, S.Wang , W.Hu , J. Cai, L. Zhang, L. Dong, L. Zhao and Y. He, Synthesis and Photocatalytic Activity of SiO_2/g-C_3N_4 Composite Photocatalyst, *Mater. Lett.*,**115,** 53

(2014).

39. Y.Wang, Z.Zhao, Y.Zhang, J. Fang, Y. Zhou, S. Yuan, C. Zhang and W. Chen, One-pot Synthesis of K-doped g-C_3N_4Nanosheets with Enhanced Photocatalytic Hydrogen Production under Visible-light Irradiation, *Appl. Surf.Sci.,* **440,**258 (2018).
40. S. Zhang, M. Li, W. Qiu, Y. Wei, G. Zhang, J. Han, H. Wang and X. Liu, Super Small Polymeric Carbon Nitride Nanospheres with Core-shell Structure for Photocatalysis, *Chemistry Select*, **2**, 10580 (2017).
41. S. W.Cao, X. F. Liu, Y. P. Yuan, Z. Y. Zhang, J. Fang, S C. J. Loo, J. Barber, T. C. Sum and C. Xue, Artificial Photosynthetic Hydrogen Evolution over g-C_3N_4Nanosheets Coupled with Cobaloxime, *Phys. Chem. Chem. Phys.,***15,** 18363 (2013).
42. W.Gao, M.Wang, C.Ran, X. Yao, H. Yang, J. Liu, D. He and J. Bai, One-pot Synthesis of Ag/r-GO/TiO_2Nanocomposites with High Solar Absorption and Enhanced Anti-recombination in Photocatalytic Applications, *Nanoscale*, **6,**5498 (2014).